AIMS Mathematics, 8(12): 31008–31021.
DOI: 10.3934/math.20231587
Received: 21 August 2023
Revised: 24 October 2023
Accepted: 02 November 2023
Published: 20 November 2023

http://www.aimspress.com/journal/Math

Research article

G^2/C^1 Hermite interpolation of offset curves of parametric regular curves

Young Joon Ahn*

Department of Mathematics Education, Chosun University, Gwangju, 61452, South Korea

* **Correspondence:** Email: ahn@chosun.ac.kr.

Abstract: In this paper we presented a method of G^2 Hermite interpolation of offset curves of regular plane curves based on approximating the normal vector fields. We showed that our approximant is also C^1 Hermite interpolation of the offset curve. Our method is capable of achieving circular precision. Another advantage of our method is that if the input curve is a polynomial curve, then our method also yields a polynomial curve. Our approximation method was applied to numerical examples and its numerical results were compared to previous offset approximation methods. It was observed that our method is almost optimal with respect to the number of control points of the approximation curves for the same tolerance.

Keywords: offset approximation; Hermite interpolation; unit normal vector field; polynomial curve; circular precision
Mathematics Subject Classification: 41A05, 65D17

1. Introduction

Approximations of offset curves by polynomial or rational parametric curves are important tasks in the fields of CAGD (computer aided geometric design) and CAD/CAM. Many offset approximation methods have been developed in the last four decades. The offset approximation method by B-spline curves using the least square method has been presented [1, 2]. A family of polynomial parametric curves, which is called the Pythagorean hodograph (PH) curve, has a rational offset [3] and it has many applications in CAGD and geometric modeling [4–10].

Offset curves of regular plane curves can be represented by the convolution of the regular plane curves and a circular arc [11, 12]. The convolution of a quadratic Bézier curve and a polynomial or rational curve is a rational curve. Based on these ideas, the offset approximation methods [11] yield rational approximation curves which are the convolution of the polynomial or rational curve and the quadratic Bézier curves interpolating the unit normal vector field of the polynomial or rational curve. The offset approximation methods by G^2 rational spline curves based on interpolating the unit normal

vector fields by G^2 quadratic splines exist [13, 14].

The notion of linear normal surfaces has been proposed to obtain their rational offsets [15, 16]. Another advantage of linear normal surfaces is that the convolutions of linear normal surfaces and general rational surfaces are always rational [17, 18], and many properties of linear normal surfaces and linear normal algebraic curves have been developed [19, 20]. The offset approximation methods that yield rational offset using linear normal curves have been presented and analyzed [21–25].

Recently, an offset approximation method of regular polynomial curves by G^1 polynomial curves based on approximating the normal vector fields of regular polynomial curves has been proposed [26]. In this paper we present the G^2/C^1 Hermite interpolation of offset curves of regular plane curves based on approximating the normal vector fields. In many applications, the G^2/C^1 interpolation is more important than the G^2/G^1 interpolation, since the latter may lead to poorly parameterized curves [27]. Our method is also capable of achieving circular precision [28, 29] as it yields the exact offset curve whenever the input curve is a circular arc. Another advantage of our method is that if the regular polynomial curve is a polynomial curve of degree n, then it also yields a polynomial curve of degree $n + 3$. We apply our offset approximation method to existing examples and illustrate that our method needs the minimum number of control points within the same tolerance.

The remainder of this paper is organized as follows. In Section 2, the preliminaries for the offset of regular plane curves and the convolution of two compatible parametric curves are introduced. In Section 3, our offset approximation method of regular plane curves is proposed and the advantages of our method are presented. We apply our method to existing examples and compare the numerical results to previous offset approximation methods in Section 4, and summarize our work in Section 5.

2. Preliminaries

In this section we present the preliminaries and notions related to the offset curves and convolution curves of regular plane curves and their approximations [11–13]. For a regular plane curve $\mathbf{x} : [a, b] \to \mathbb{R}^2$,

$$\mathbf{T}(t) = \frac{\mathbf{x}'(t)}{\|\mathbf{x}'(t)\|} \text{ and } \mathbf{N}(t) = R\mathbf{T}(t) \tag{2.1}$$

are the unit tangent and normal vectors of $\mathbf{x}$ at the point $\mathbf{x}(t)$, respectively, where R denotes the ninety degree clockwise rotation operator. The curve $\mathbf{x} + r\mathbf{N} : [a, b] \to \mathbb{R}^2$ is called the offset curve of $\mathbf{x}$ with the offset distance $r \in \mathbb{R}$.

Two curves $\mathbf{x}_1$ and $\mathbf{x}_2$ are said to be compatible [12, 30] if there exists a reparametrization $s = s(t)$ satisfying $\mathbf{x}_1'(t) \parallel \mathbf{x}_2'(s(t))$ and $\langle \mathbf{x}_1'(t), \mathbf{x}_2'(s(t)) \rangle > 0$. The convolution curve $\mathbf{x}_1 * \mathbf{x}_2$ for two compatible curves $\mathbf{x}_1$, $\mathbf{x}_2$ is defined by

$$(\mathbf{x}_1 * \mathbf{x}_2)(t) = \mathbf{x}_1(t) + \mathbf{x}_2(s(t)).$$

The offset curve $\mathbf{x} + r\mathbf{N}$ of $\mathbf{x}$ with offset distance r can be represented by $\mathbf{x} * r\mathbf{N}$, i.e.,

$$\mathbf{x}(t) + r\mathbf{N}(t) = (\mathbf{x} * r\mathbf{N})(t),$$

since two curves $\mathbf{x}$ and $r\mathbf{N}$ are compatible [11, 12].

The Hausdorff distance between two curves $\mathbf{x}_1 : [a, b] \to \mathbb{R}^3$ and $\mathbf{x}_2 : [c, d] \to \mathbb{R}^3$ is defined by

$$d_H(\mathbf{x}_1, \mathbf{x}_2) = \max\left(\max_{t\in[a,b]} \min_{s\in[c,d]} \|\mathbf{x}_1(t) - \mathbf{x}_2(s)\|, \max_{s\in[c,d]} \min_{t\in[a,b]} \|\mathbf{x}_1(t) - \mathbf{x}_2(s)\| \right).$$

The Hausdorff distance between a circular arc and a general plane curve is easier to be obtained than that between two general plane curves [11,31–33]. For the unit normal vector $\mathbf{N}$ of a plane curve $\mathbf{x}$ and its approximant $\mathbf{N}^a$, the Hausdorff distance is invariant under convolution, i.e.,

$$d_H(\mathbf{x} * r\mathbf{N}, \mathbf{x} * r\mathbf{N}^a) = r d_H(\mathbf{N}, \mathbf{N}^a) \tag{2.2}$$

if these curves are regular [13].

3. G^2 Hermite interpolation of offset curve of regular plane curve

In this section, we present a G^2/C^1 Hermite interpolation of offset curves of regular parametric plane curves based on approximating the normal vector field. Let $\mathbf{x} : [0,1] \to \mathbb{R}^2$ be a regular parametric plane curve. Let $\mathbf{N} : [0,1] \to \mathbb{R}^2$ be the unit normal vector field of $\mathbf{x}$ as in (2.1). We propose its approximant $\mathbf{N}^a : [0,1] \to \mathbb{R}^2$ by

$$\mathbf{N}^a(t) = \int_0^t \mathbf{x}'(u)\alpha(u)du + \mathbf{N}(0), \tag{3.1}$$

where $\alpha : [0,1] \to \mathbb{R}$ is a cubic polynomial defined by

$$\alpha(t) = \sum_{i=0}^{3} \alpha_i B_i^3(t),$$

and $B_i^n(t) = \binom{n}{i} t^i (1-t)^{n-i}$, $0 \le i \le n$, are the Bernstein polynomials of degree n. The reason why $\mathbf{N}^a$ is chosen as in Eq (3.1) is that if the derivatives of $\mathbf{N}^a$ and $\mathbf{x}$ for the same parameter are parallel, then their convolution can be directly obtained by their simple addition. This method was originally presented by Ahn and Hoffmann [21], and Kim et al. [26] used a similar equation to Eq (3.1), which is a special case of our method. In this paper, the coefficients $\alpha_0, \alpha_1, \alpha_2, \alpha_3$ in Eq (3.1) are determined such that $\mathbf{N}^a$ is a G^2 Hermite interpolation of $\mathbf{N}$. Accordingly, we show that the approximation $\mathbf{x} * r\mathbf{N}^a$ is a G^2 Hermite interpolation of the offset curve $\mathbf{x} * r\mathbf{N}$ with the offset distance $r \in \mathbb{R}$.

Since $\mathbf{N}^a(0) = \mathbf{N}(0)$ in (3.1), the curve $\mathbf{N}^a$ is a G^0 Hermite interpolation of $\mathbf{N}$ if $\mathbf{N}^a(1) = \mathbf{N}(1)$ holds. It follows from $\mathbf{N}^a(1) = \mathbf{N}(1)$ that

$$\sum_{i=1}^{2} \int_0^1 \mathbf{x}'(t) B_i^3(t) dt \alpha_i = (\mathbf{N}(1) - \mathbf{N}(0)) - \sum_{i=0}^{1} \int_0^1 \mathbf{x}'(t) B_{3i}^3(t) dt \alpha_{3i}. \tag{3.2}$$

This is a linear equation with respect to α_1 and α_2, i.e., (3.2) can be represented by

$$\mathbf{v}_1\alpha_1 + \mathbf{v}_2\alpha_2 = \mathbf{v},$$

where

$$\mathbf{v}_i = \int_0^1 \mathbf{x}'(t) B_i^3(t) dt, \quad i = 1, 2, \tag{3.3}$$

and $\mathbf{v}$ denotes the right side of (3.2). The linear equation in (3.2) for α_1 and α_2 has a unique solution,

$$\alpha_1 = \frac{\mathbf{v} \times \mathbf{v}_2}{\mathbf{v}_1 \times \mathbf{v}_2}, \quad \alpha_2 = \frac{\mathbf{v}_1 \times \mathbf{v}}{\mathbf{v}_1 \times \mathbf{v}_2}, \tag{3.4}$$

if $\mathbf{x}$ is convex and the length of the curve $\mathbf{N} : [0,1] \to S^1$ is less than π, where $(x_1, y_1) \times (x_2, y_2) = x_1y_2 - x_2y_1$, and S^1 is the unit circle centered at the origin in $\mathbb{R}^2$.

Proposition 3.1. *If* $\mathbf{x}$ *is convex and the length of the curve* $\mathbf{N}$ *is less than* π*, then the linear equation in (3.2) for* α_1 *and* α_2 *has a unique solution as in (3.4).*

Proof. For convenience, the notation $\arg \mathbf{u}$ for a vector $\mathbf{u} = (u_1, u_2)$ is used to the argument of the complex number $u_1 + \mathrm{i}u_2$, i.e., $\arg \mathbf{u} = \arg(u_1 + \mathrm{i}u_2)$. We may assume that $\mathbf{x}$ is turning left and $\arg \mathbf{x}'(0) = 0$, then $\arg \mathbf{x}'(t)$ is increasing and $\arg \mathbf{x}'(t) \in [0, \pi)$. Since

$$\arg \int_0^1 \mathbf{x}'(t)(1-t)dt < \arg \int_0^1 \mathbf{x}'(t)tdt,$$

we have

$$\arg \int_0^1 \mathbf{x}'(t)B_1^3(t)dt < \arg \int_0^1 \mathbf{x}'(t)B_2^3(t)dt,$$

and $\mathbf{v}_1$ and $\mathbf{v}_2$ are linearly independent. Thus, the assertion follows. □

From now on we assume that the regular parametric curve $\mathbf{x}$ satisfies the assumption of Proposition 3.1. If not, we can make $\mathbf{x}$ satisfy the assumption by subdivisions at inflection points and bisections of $\mathbf{x}$. The approximation curve $\mathbf{N}^a$ with α_1, α_2 satisfying (3.4) is a G^0 Hermite interpolation of $\mathbf{N}$. Now, we find the two coefficients α_0, α_3 such that $\mathbf{N}^a$ is a G^2 Hermite interpolation of $\mathbf{N}$. Let $\kappa_{\mathbf{x}}(t)$ be the signed curvature of $\mathbf{x}$ at the point $\mathbf{x}(t)$.

Proposition 3.2. *The two curves* $\mathbf{N}^a$ *and* $\mathbf{N}$ *have the same signed curvature at both endpoints if and only if* $|\alpha_{3i}| = |\kappa_{\mathbf{x}}(i)|$*,* $i = 0, 1$*.*

Proof. It follows from (3.1) that

$$\mathbf{N}^{a\prime}(i) = \alpha_{3i}\mathbf{x}'(i), \quad \mathbf{N}^{a\prime\prime}(i) = \alpha_{3i}\mathbf{x}''(i) + 3\Delta\alpha_{2i}\mathbf{x}'(i), \tag{3.5}$$

for $i = 0, 1$, where $\Delta\alpha_i = \alpha_{i+1} - \alpha_i$. Thus, we have

$$\mathbf{N}^{a\prime}(i) \times \mathbf{N}^{a\prime\prime}(i) = \alpha_{3i}^2 \mathbf{x}'(i) \times \mathbf{x}''(i), \tag{3.6}$$

$i = 0, 1$, and

$$\kappa_{\mathbf{N}^a}(i) = \frac{\mathbf{N}^{a\prime}(i) \times \mathbf{N}^{a\prime\prime}(i)}{||\mathbf{N}^{a\prime}(i)||^3} = \frac{\mathbf{x}'(i) \times \mathbf{x}''(i)}{|\alpha_{3i}|\,||\mathbf{x}'(i)||^3} = \frac{\kappa_{\mathbf{x}}(i)}{|\alpha_{3i}|}.$$

Hence $\kappa_{\mathbf{N}^a}(i) = \kappa_{\mathbf{N}}(i)$, $i = 0, 1$ if and only if $\kappa_{\mathbf{x}}(i) = \kappa_{\mathbf{N}}(i)|\alpha_{3i}|$. If $\mathbf{x}$ is turning left or right, then the signed curvature of $\mathbf{N}$ is one or negative one, respectively. Therefore, $\kappa_{\mathbf{x}}(i) = \kappa_{\mathbf{N}}(i)|\alpha_{3i}|$, $i = 0, 1$ is equivalent to $|\alpha_{3i}| = |\kappa_{\mathbf{x}}(i)|$. □

We have two choices of $\alpha_{3i} = \pm\kappa_{\mathbf{x}}(i)$, $i = 0, 1$. From (2.1) it follows that

$$\mathbf{N}'(i) = \frac{(\mathbf{x}'(i) \times \mathbf{x}''(i))\mathbf{x}'(i)}{||\mathbf{x}'(i)||^3} = \kappa_{\mathbf{x}}(i)\mathbf{x}'(i). \tag{3.7}$$

Thus, if $\alpha_{3i} = -\kappa_{\mathbf{x}}(i)$, then

$$\mathbf{N}^{a\prime}(i) = \alpha_{3i}\mathbf{x}'(i) = -\kappa_{\mathbf{x}}(i)\mathbf{x}'(i) = -\mathbf{N}'(i),$$

which implies that $\mathbf{N}^a$ has the opposite tangent direction of $\mathbf{N}$ at both endpoints. Hence, we choose $\alpha_{3i} = \kappa_{\mathbf{x}}(i)$, $i = 0, 1$ for the G^2 Hermite interpolation $\mathbf{N}^a$ of $\mathbf{N}$. The approximant $\mathbf{N}^a$ is constructed by α_1, α_2, satisfying (3.4) and by

$$\alpha_{3i} = \kappa_{\mathbf{x}}(i) = \frac{\mathbf{x}'(i) \times \mathbf{x}''(i)}{\|\mathbf{x}'(i)\|^3}, \quad i = 0, 1. \tag{3.8}$$

Now, we show that the curve $\mathbf{x} + r\mathbf{N}^a$ is a C^1 and G^2 Hermite interpolation of the offset curve $\mathbf{x} + r\mathbf{N}$ as follows.

Proposition 3.3. *The approximant $\mathbf{x} + r\mathbf{N}^a$ is a C^1 and G^2 Hermite interpolation of the offset curve $\mathbf{x} + r\mathbf{N}$.*

Proof. Since $\mathbf{N}^a(i) = \mathbf{N}(i)$, $i = 0, 1$, we have $(\mathbf{x} + r\mathbf{N}^a)(i) = (\mathbf{x} + r\mathbf{N})(i)$. It follows from (3.5), (3.7) and (3.8) that

$$\mathbf{N}^{a\prime}(i) = \mathbf{N}'(i), \quad i = 0, 1. \tag{3.9}$$

Thus, we obtain

$$(\mathbf{x} + r\mathbf{N}^a)'(i) = (\mathbf{x} + r\mathbf{N})'(i), \quad i = 0, 1, \tag{3.10}$$

which implies that $\mathbf{x} + r\mathbf{N}^a$ is a C^1 Hermite interpolation of the offset curve $\mathbf{x} + r\mathbf{N}$.

Since the curve $\mathbf{N}$ is a circular arc, we have

$$\mathbf{N}'(i) \times \mathbf{N}''(i) = sgn(\mathbf{N}'(i) \times \mathbf{N}''(i))\|\mathbf{N}'(i)\|^3, \tag{3.11}$$

$i = 0, 1$. It follows from (3.6)–(3.9) and (3.11) that

$$\begin{aligned} \mathbf{N}^{a\prime}(i) \times \mathbf{N}^{a\prime\prime}(i) &= \alpha_{3i}^2 \mathbf{x}(i) \times \mathbf{x}''(i) = (\kappa_{\mathbf{x}}(i))^3 \|\mathbf{x}'(i)\|^3 = \mathbf{N}'(i) \times \mathbf{N}''(i), \\ \mathbf{x}'(i) \times \mathbf{N}^{a\prime\prime}(i) &= \frac{\mathbf{N}^{a\prime}(i) \times \mathbf{N}^{a\prime\prime}(i)}{\kappa_{\mathbf{x}}(i)} = \frac{\mathbf{N}'(i) \times \mathbf{N}''(i)}{\kappa_{\mathbf{x}}(i)} = \mathbf{x}'(i) \times \mathbf{N}''(i). \end{aligned} \tag{3.12}$$

By (3.9) and (3.12), we obtain

$$(\mathbf{x}'(i) + r\mathbf{N}^{a\prime}(i)) \times (\mathbf{x}''(i) + r\mathbf{N}^{a\prime\prime}(i)) = (\mathbf{x}'(i) + r\mathbf{N}'(i)) \times (\mathbf{x}''(i) + r\mathbf{N}''(i)),$$

$i = 0, 1$ and (3.10) implies that $\mathbf{x} + r\mathbf{N}^a$ is a G^2 Hermite interpolation of $\mathbf{x} + r\mathbf{N}$. □

3.1. Circular precision

In this section we show that if the regular parametric curve $\mathbf{x}$ is a circular arc, then our approximation method yields the exact offset curve.

Let $\mathbf{x}$ be a circular arc represented by

$$\mathbf{x}(t) = \mathbf{c}_0 + \gamma(\cos(t_0 + lt), \sin(t_0 + lt)), \quad t \in [0, 1],$$

where $\mathbf{c}_0 \in \mathbb{R}^2$, $\gamma > 0$ and $l \in (0, \pi)$ are the center, radius, and length of the circular arc, respectively. By (3.8), we have $\alpha_0 = \alpha_3 = 1/\gamma$. The unit normal vector $\mathbf{N}$ satisfies $\mathbf{N}(t) = \frac{1}{\gamma}(\mathbf{x}(t) - \mathbf{c}_0)$ and (3.3) yields

$$\mathbf{v}_1 = 3\gamma\left(\frac{R\mathbf{N}(0)}{l} - \frac{4\mathbf{N}(0) + 2\mathbf{N}(1)}{l^2} - \frac{6R(\mathbf{N}(0) - \mathbf{N}(1))}{l^3}\right),$$

$$\mathbf{v}_2 = 3\gamma\left(\frac{R\mathbf{N}(1)}{l} + \frac{2\mathbf{N}(0) + 4\mathbf{N}(1)}{l^2} + \frac{6R(\mathbf{N}(0) - \mathbf{N}(1))}{l^3}\right).$$

It follows from the definition of $\mathbf{v}$ and (3.2) that

$$\mathbf{v} = 3\left(\frac{R(\mathbf{N}(0) + \mathbf{N}(1))}{l} - \frac{2(\mathbf{N}(0) - \mathbf{N}(1))}{l^2}\right).$$

Thus we obtain

$$\begin{aligned}
\mathbf{v}_1 \times \mathbf{v}_2 &= 9\gamma^2\left(\frac{\mathbf{N}(0) \times \mathbf{N}(1)}{l^2} + \frac{4 - 8(\mathbf{N}(0) \times R\mathbf{N}(1))}{l^3}\right. \\
&\quad \left. -24\frac{\mathbf{N}(0) \times \mathbf{N}(1)}{l^4} + 24\frac{1 + \mathbf{N}(0) \times R\mathbf{N}(1)}{l^5}\right), \\
\mathbf{v} \times \mathbf{v}_2 &= \mathbf{v}_1 \times \mathbf{v} = 9\gamma\left(\frac{\mathbf{N}(0) \times \mathbf{N}(1)}{l^2} + \frac{4 - 8(\mathbf{N}(0) \times R\mathbf{N}(1))}{l^3}\right. \\
&\quad \left. -24\frac{\mathbf{N}(0) \times \mathbf{N}(1)}{l^4} + 24\frac{1 + \mathbf{N}(0) \times R\mathbf{N}(1)}{l^5}\right).
\end{aligned}$$

Hence $\alpha_1 = \alpha_2 = 1/\gamma$, and $\alpha(t) = 1/\gamma$ for all $t \in [0, 1]$. Equation (3.1) yields

$$\mathbf{N}^a(t) = \frac{1}{\gamma}\int_0^t \mathbf{x}'(u)du + \mathbf{N}(0) = \mathbf{N}(t),$$

for all $t \in [0, 1]$. Therefore, our method yields the exact offset curve for the circular arc $\mathbf{x}$.

3.2. G^2/C^1 Hermite interpolation of offset curve of parametric polynomial curves

An advantage of our method is that if $\mathbf{x}$ is a regular polynomial curve, then our method yields a polynomial approximant for a G^2/C^1 Hermite interpolation of the offset of $\mathbf{x}$. Let $\mathbf{x} : [0, 1] \to \mathbb{R}^2$ be the parametric polynomial curve of degree n represented in Bézier form

$$\mathbf{x}(t) = \sum_{j=0}^{n} \mathbf{b}_j B_j^n(t),$$

where $\mathbf{b}_j$, $j = 0, 1, \ldots, n$, are the control points of $\mathbf{x}$. From (3.1) it follows that

$$\mathbf{N}^a(t) = \int_0^t \mathbf{x}'(u) \sum_{i=0}^{3} \alpha_i B_i^3(u)du + \mathbf{N}(0), \tag{3.13}$$

which is a polynomial curve of degree $n + 3$ and G^2/C^1 Hermite interpolation of $\mathbf{N}$. Since $(\mathbf{N}^a)'(t) \parallel \mathbf{x}'(t)$, $t \in [0, 1]$, the offset curve is obtained by

$$(\mathbf{x} * r\mathbf{N}^a)(t) = \mathbf{x}(t) + r\mathbf{N}^a(t),$$

which is also a polynomial curve and its degree is $n + 3$.

In the rest of this section, we obtain the cubic polynomial $\alpha(t)$ in the form of control points of $\mathbf{x}$. Note that (3.8) yields

$$\alpha_0 = \frac{n-1}{n}\frac{\Delta\mathbf{b}_0 \times \Delta\mathbf{b}_1}{\|\Delta\mathbf{b}_0\|^3}, \quad \alpha_3 = \frac{n-1}{n}\frac{\Delta\mathbf{b}_{n-2} \times \Delta\mathbf{b}_{n-1}}{\|\Delta\mathbf{b}_{n-1}\|^3}.$$

Using three formulas [34, 35]

$$\begin{aligned} \mathbf{x}'(t) &= \sum_{j=0}^{n-1} n\Delta\mathbf{b}_j B_j^{n-1}(t), \\ B_j^{n-1}(u)B_i^3(u) &= \frac{\binom{n-1}{j}\binom{3}{i}}{\binom{n+2}{i+j}} B_{i+j}^{n+2}(u), \\ \int_0^1 B_k^{n+2}(u)du &= \frac{1}{n+3}, \quad k = 0, 1, \ldots, n+2, \end{aligned}$$

we have

$$\int_0^1 \mathbf{x}'(u) \sum_{i=0}^{3} \alpha_i B_i^3(u)du = \frac{n}{n+3} \sum_{j=0}^{n-1}\sum_{i=0}^{3} \frac{\binom{n-1}{j}\binom{3}{i}}{\binom{n+2}{i+j}} \alpha_i \Delta\mathbf{b}_j.$$

Equation (3.2) and the definition of $\mathbf{v}$ yield

$$\begin{aligned} \mathbf{v}_i &= \frac{3n}{n+3} \sum_{j=0}^{n-1} \frac{\binom{n-1}{j}}{\binom{n+2}{i+j}} \Delta\mathbf{b}_j, \quad i = 1, 2, \\ \mathbf{v} &= \mathbf{N}(1) - \mathbf{N}(0) - \frac{n}{n+3} \sum_{j=0}^{n-1} \left(\frac{\alpha_0}{\binom{n+2}{j}} + \frac{\alpha_3}{\binom{n+2}{3+j}} \right) \binom{n-1}{j} \Delta\mathbf{b}_j. \end{aligned}$$

Thus, the coefficients α_1 and α_2 are obtained from (3.4) in the form of control points $\mathbf{b}_j$ of $\mathbf{x}$.

4. Numerical examples and comparison

In this section we describe our approximation method and apply it to examples in the literature. The numerical results of our method are compared to those of previous methods.

Our approximation method yields the curvature continuous polynomial spline curve of degree $n+3$ approximating the offset of the input curve when it is a polynomial spline curve of degree n. In our approximation method, the input curve $\mathbf{x}$ is first subdivided such that each subdivided segment becomes a convex polynomial segment. We use the divide-and-conquer method. If the Hausdorff distance between the offset approximant and the offset of the polynomial segment is larger than the tolerance, then the segment is subdivided into two segments. The offset curves are approximated separately as shown in Figure 1. This process is repeated until the error is less than the tolerance.

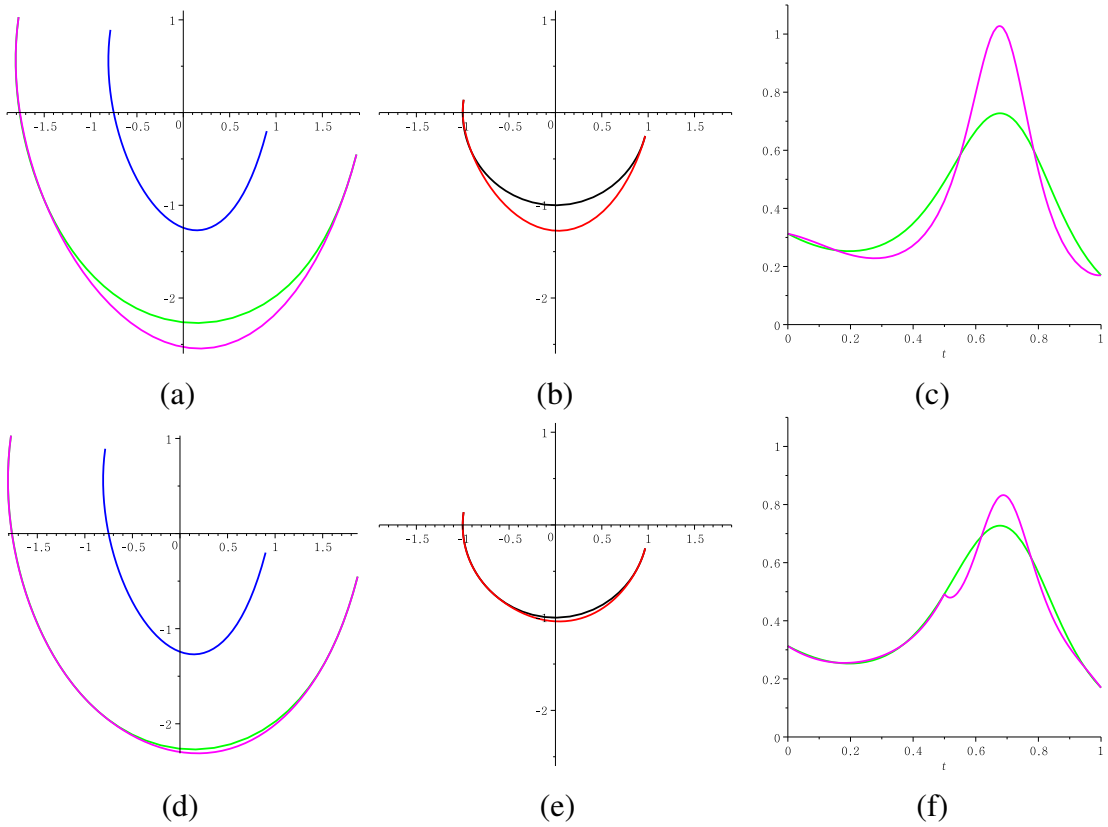

Figure 1. (a) Offset curve $\mathbf{x} + \mathbf{N}$ (green-color) of the cubic Bézier curve $\mathbf{x}$ (blue) and our approximation curve $\mathbf{x} + \mathbf{N}^a$ (magenta) whose error is larger than 10^{-1}. (b) Unit normal vector $\mathbf{N}$ (black) and our approximant $\mathbf{N}^a$ (red). (c) Curvatures of $\mathbf{x} + \mathbf{N}$ (green) and $\mathbf{x} + \mathbf{N}^a$ (magenta). (d)–(f) After one subdivision at the parametric midpoint, the error is less than 10^{-1} and the curvature of the approximant is continuous.

The Hausdorff distance between two curves $\mathbf{x} + r\mathbf{N}$ and $\mathbf{x} + r\mathbf{N}^a$ can be measured by (2.2), because $\mathbf{x}+r\mathbf{N} = \mathbf{x}*r\mathbf{N}$ and $\mathbf{x}+r\mathbf{N}^a = \mathbf{x}*r\mathbf{N}^a$. Since $\mathbf{N}$ is a circular arc and $\mathbf{N}^a$ is a polynomial parametric curve, it is easy to calculate $d_H(\mathbf{N}, \mathbf{N}^a)$, which is an advantage of the offset approximation method based on approximating the unit normal vector field [11, 13].

Subsequently, our offset approximation method is applied to three numerical examples. The first and second examples are the offset approximations of the cubic Bézier and B-spline curves as shown in Figures 1 and 2, respectively, which were originally presented by Lee et al. [11]. The numerical results obtained by the previous methods can be found in Tables 1 and 2, which have been presented in [11, 13, 26], except for the data of the 'CL' method in Table 2. In this paper, our results are added to the last columns of the tables and the data of the CL method in Table 2 is newly added. It can be observed that our approximation method yields the optimal approximation, except for the 'Lst' method with respect to the number of control points within the same tolerance. The Lst method was proposed by Lee et al. [11] and they explained that it is an extension of Hoschek and Wissel [2] while adapting the global error bounding technique of the method in [36].

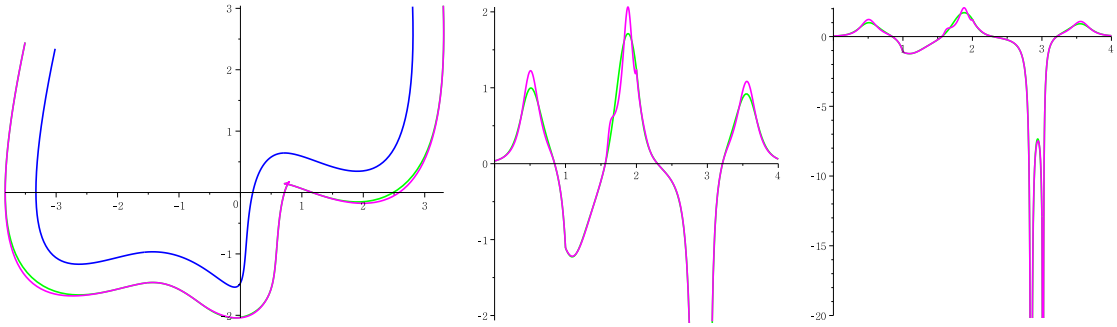

(a) (b) (c)

Figure 2. (a) Cubic B-spline curve composed of four Bézier curves with C^2 continuity (blue color), its offset curve (green), and our approximant (magenta) composed of 10 polynomial curves of degree six with G^2 continuity and error less than 10^{-1}. (b)–(c) Curvature plots of the offset curve (green) and our approximant (magenta).

Table 1. Minimum number of control points needed for offset approximation methods with errors less than the given tolerance TOL for the cubic Bézier curve in Figure 1.

TOL	*Lst* [2, 11, 36]	*M2* [11]	*CL* [21]	*QS* [14]	*QL* [22]	[26]	Our method
10^{-1}	7	22	10	15	23	13	13
10^{-2}	13	29	16	22	34	21	19
10^{-3}	19	43	28	43	45	33	31
10^{-4}	31	71	43	71	56	57	43
10^{-5}	50	127	79	120	78	105	61

Table 2. Minimum number of control points needed for offset approximation methods with errors less than TOL for the cubic B-spline curve in Figure 2.

TOL	*Lst* [2, 11, 36]	*M2* [11]	*CL* [21]	*QS* [14]	*QL* [22]	[26]	Our method
10^{-1}	16	78	37	85	111	49	61
10^{-2}	48	92	55	92	133	61	79
10^{-3}	84	120	100	134	144	109	103
10^{-4}	138	176	175	204	177	168	151
10^{-5}	240	302	310	316	243	289	199

The third example is an offset approximation of boundaries of the character 'S', and its left and right boundaries are composed of seven and six Bézier curves of degree three, respectively. This example was proposed by Kim et al. [26] and their numerical results are presented in the fifth column of Table 3. For the example, we have added all the data that we could obtain from the previous methods in Table 3. We have also added our numerical results to the last column of Table 3 for comparison with those of the previous methods. As shown in Figure 3, the approximation curve has self-intersections. In many practical applications of planar curve offsetting, the self-intersection loops need to be removed [37]. Actually, the self-intersections of our approximation curve are the intersections

of two Bézier segments. Many methods for finding the intersection points of two parametric curves have been presented [38–40]. The trimmed curve of our approximant can be obtained by finding the intersection points and eliminating the intersection loops as shown in Figure 4.

Table 3. Minimum number of control points needed for offset approximation methods with errors less than TOL for the left and right boundaries of the character 'S' in Figure 3.

Left boundary					
TOL	CL [21]	QS [14]	QL [22]	[26]	Our method
10^{-1}	46	106	111	45	61
10^{-2}	88	134	144	85	85
10^{-3}	157	197	188	121	103
10^{-4}	289	323	254	217	163
10^{-5}	496	526	331	373	241
Right boundary					
TOL	CL [21]	QS [14]	QL [22]	[26]	Our method
10^{-1}	49	113	111	41	61
10^{-2}	91	141	155	77	79
10^{-3}	166	218	199	133	109
10^{-4}	310	337	254	225	163
10^{-5}	553	540	309	389	229

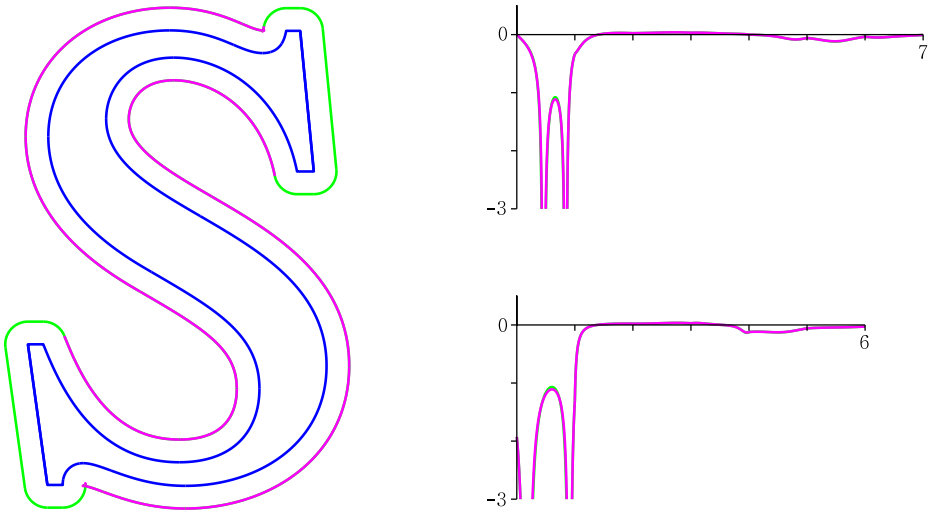

Figure 3. Left: Character 'S' (blue color) composed of 13 cubic Bézier curves and six line segments, its offset curve (green) and our approximant (magenta) composed of 20 polynomial curves of degree six with its error less than 10^{-1}. Right top: Curvature plots of the offset curve (green) for the left boundary curve composed of seven cubic Bézier curves and our approximant (magenta). Right bottom: Curvature plots of the offset curve (green) for the right boundary curve composed of six cubic Bézier curves and our approximant (magenta).

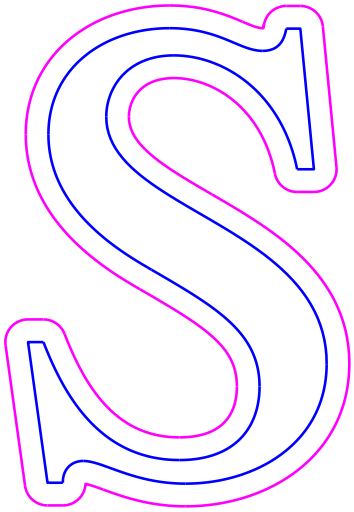

Figure 4. Trimmed offset approximation curve of the character 'S'. The offset curves of corner points are circular arcs, which can be approximated by Bézier curves of degree six with high precision [33, 41].

For all examples, the curvatures of the offset curve and our approximant are plotted in Figures 1–3, and we can see the curvature continuity of our offset approximant.

5. Conclusions

In this paper we presented the offset approximation method for regular plane parametric curves. Our method has a few advantages. It yields the G^2 and C^1 Hermite interpolation of the offset curve. The method achieves circular precision and yields a polynomial approximant for the offset curve whenever the input curve is a polynomial curve. Our method facilitates the calculation of the error since it is based on approximating the unit normal vector field. Our method also has the smallest error from almost all previous offset approximation methods, with respect to the number of control points within the same tolerance.

Use of AI tools declaration

The authors declare they have not used Artificial Intelligence (AI) tools in the creation of this article.

Acknowledgments

This study was supported by research funds from Chosun University, 2023 and by Basic Science Research Program through the National Research Foundation of Korea (NRF) funded by the Ministry of Education (NRF-2021R1F1A1045830).

Conflict of interest

The authors declare no conflict of interest.

References

1. J. Hoschek, Spline approximation of offset curves, *Comput. Aided Geom. Design*, **5** (1988), 33–40. https://doi.org/10.1016/0167-8396(88)90018-0
2. J. Hoschek, N. Wissel, Optimal approximate conversion of spline curves and spline approximation of offset curves, *Comput. Aided Design*, **20** (1988), 475–483. https://doi.org/10.1016/0010-4485(88)90006-1
3. R. T. Farouki, C. A. Neff, Analytic properties of plane offset curves, *Comput. Aided Geom. Design*, **7** (1990), 83–99. https://doi.org/10.1016/0167-8396(90)90023-K
4. L. Fang, Y. Li, Algebraic and geometric characterizations of a class of algebraic-hyperbolic Pythagorean-hodograph curves, *Comput. Aided Geom. Design*, **97** (2022), 102121. https://doi.org/10.1016/j.cagd.2022.102121
5. R. T. Farouki, M. Knez, V. Vitrih, E. Žagar, On the construction of polynomial minimal surfaces with Pythagorean normals, *Appl. Math. Comput.*, **435** (2022), 127439. https://doi.org/10.1016/j.amc.2022.127439
6. G. Cigler, E. Žagar, Interpolation of planar G^1 data by Pythagorean-hodograph cubic biarcs with prescribed arc lengths, *Comput. Aided Geom. Design*, **96** (2022), 102119. https://doi.org/10.1016/j.cagd.2022.102119
7. M. Knez, F. Pelosi, M. L. Sampoli, Construction of G^2 planar Hermite interpolants with prescribed arc lengths, *Appl. Math. Comput.*, **426** (2022), 127092. https://doi.org/10.1016/j.amc.2022.127092
8. R. T. Farouki, F. Pelosi, M. L. Sampoli, Construction of planar quintic Pythagorean-hodograph curves by control-polygon constraints, *Comput. Aided Geom. Design*, **103** (2023), 102192. https://doi.org/10.1016/j.cagd.2023.102192
9. H. P. Schröcker, Z. Šír. Partial fraction decomposition for rational Pythagorean hodograph curves, *J. Comput. Appl. Math.*, **428** (2023), 115196. https://doi.org/10.1016/j.cam.2023.115196
10. E. Žagar, Arc length preserving G^2 Hermite interpolation of circular arcs, *J. Comput. Appl. Math.*, **424** (2023), 115008. https://doi.org/10.1016/j.cam.2022.115008
11. I. K. Lee, M. S. Kim, G. Elber, Planar curve offset based on circle approximation, *Comput. Aided Design*, **28** (1996), 617–630. https://doi.org/10.1016/0010-4485(95)00078-X
12. I. K. Lee, M. S. Kim, G. Elber, Polynomial/rational approximation of Minkowski sum boundary curves, *Grap. Models Image Process.*, **60** (1998), 136–165. https://doi.org/10.1006/gmip.1998.0464
13. Y. J. Ahn, C. M. Hoffmann, Y. S. Kim, Curvature-continuous offset approximation based on circle approximation using quadratic Bézier biarcs, *Comput. Aided Design*, **43** (2011), 1011–1017. https://doi.org/10.1016/j.cad.2011.04.005
14. S. W. Kim, S. C. Bae, Y. J. Ahn, An algorithm for G^2 offset approximation based on circle approximation by G^2 quadratic spline, *Comput. Aided Design*, **73** (2016), 36–40. https://doi.org/10.1016/j.cad.2015.11.003
15. B. Jüttler, Triangular Bézier surface patches with a linear normal vector field, In: *The mathematics of surfaces VIII, information geometers*, Winchester, 1998.

16. B. Jüttler, M. L. Sampoli. Hermite interpolation by piecewise polynomial surfaces with rational offsets, *Comput. Aided Geom. Design*, **17** (2000), 361–385. https://doi.org/10.1016/S0167-8396(00)00002-9

17. M. Sampoli, M. Peternell, B. Jüttler. Rational surfaces with linear normals and their convolutions with rational surfaces, *Comput. Aided Geom. Design*, **23** (2006), 179–192. https://doi.org/10.1016/j.cagd.2005.07.001

18. M. Peternell, B. Odehnal, Convolution surfaces of quadratic triangular Bézier surfaces, *Comput. Aided Geom. Design*, **25** (2008), 116–129. https://doi.org/10.1016/j.cagd.2007.05.003

19. Z. Šír, J. Gravesen, B. Jüttler, Curves and surfaces represented by polynomial support functions, *Theor. Comput. Sci.*, **392** (2008), 141–157. https://doi.org/10.1016/j.tcs.2007.10.009

20. J. Vršek, M. Lávička, Exploring hypersurfaces with offset-like convolutions, *Comput. Aided Geom. Design*, **29** (2012), 676–690. https://doi.org/10.1016/j.cagd.2012.07.002

21. Y. J. Ahn, C. M. Hoffmann, Approximate convolution with pairs of cubic Bézier LN curves, *Comput. Aided Geom. Design*, **28** (2011), 357–367. https://doi.org/10.1016/j.cagd.2011.06.006

22. Y. J. Ahn, C. M. Hoffmann, Circle approximation using LN Bézier curves of even degree and its application, *J. Math. Anal. Appl.*, **40** (2014), 257–266. https://doi.org/10.1016/j.jmaa.2013.07.079

23. X. J. Lu, J. Zheng, Y. Cai, G. Zhao, Geometric characteristics of a class of cubic curves with rational offsets, *Comput. Aided Design*, **70** (2016), 36–45. https://doi.org/10.1016/j.cad.2015.07.006

24. Y. J. Ahn, C. M. Hoffmann, Sequence of G^n LN polynomial curves approximating circular arcs, *J. Comp. Appl. Math.*, **341** (2018), 117–126. https://doi.org/10.1016/j.cam.2018.03.028

25. Y. J. Ahn, C. M. Hoffmann, G^2 Hermite interpolation with quartic regular linear normal curves, *J. Comp. Appl. Math.*, **424** (2023), 114981. https://doi.org/10.1016/j.cam.2022.114981

26. S. W. Kim, R. Lee, Y. J. Ahn, A new method approximating offset curve by Bézier curve using parallel derivative curves, *Comp. Appl. Math.*, **37** (2018), 2053–2064. https://doi.org/10.1007/s40314-017-0437-x

27. G. Albrecht, C. V. Beccari, L. Romani, G^2/C^1 Hermite interpolation by planar PH B-spline curves with shape parameter, *Appl. Math. Lett.*, **121** (2021), 107452. https://doi.org/10.1016/j.aml.2021.107452

28. G. Farin, Geometric Hermite interpolation with circular precision, *Comput. Aided Geom. Design*, **40** (2008), 476–479. https://doi.org/10.1016/j.cad.2008.01.003

29. D. J. Walton, D. S. Meek, G^2 Hermite interpolation with circular precision, *Comput. Aided Design*, **42** (2010), 749–758. https://doi.org/10.1016/j.cad.2010.04.004

30. R. Lee, Y. J. Ahn, Geometric shape analysis for convolution curve of two compatible quadratic Bézier curves, *J. Comput. Appl. Math.*, **288** (2015), 141–150. https://doi.org/10.1016/j.cam.2015.04.012

31. T. Dokken, M. Dæhlen, T. Lyche, K. Mørken, Good approximation of circles by curvature-continuous Bézier curves, *Comput. Aided Geom. Design*, **7** (1990), 33–41. https://doi.org/10.1016/0167-8396(90)90019-N

32. Y. J. Ahn, C. M. Hoffmann, Offset approximation of polygons on an ellipsoid, *Acta Geod. Geophys.*, **56** (2021), 293–302. https://doi.org/10.1007/s40328-021-00335-7

33. H. M. Yoon, Y. J. Ahn, Circular arc approximation by hexic polynomial curves, *Comput. Appl. Math.*, **42** (2023), 256. https://doi.org/10.1007/s40314-023-02315-9

34. G. Farin, *Curves and surfaces for CAGD: A practical guide*, San Francisco: Morgan-Kaufmann, 2002.

35. B. G. Lee, Y. Park, J. Yoo, Application of Legendre-Bernstein basis transformations to degree elevation and degree reduction, *Comput. Aided Geom. Design*, **19** (2002), 709–718. https://doi.org/10.1016/S0167-8396(02)00164-4

36. G. Elber, E. Cohen, Error bounded variable distance offset perator for free form curves and surfaces, *Int. J. Comput. Geom. Appl.*, **1** (1991), 67–78. https://doi.org/10.1142/S0218195991000062

37. T. Maekawa, N. M. Patrikalakis, Computation of singularities and intersections of offsets of planar curves, *Comput. Aided Geom. Design*, **10** (1993), 407–429. https://doi.org/10.1016/0167-8396(93)90020-4

38. T. W. Sederberg, T. Nishita, Curve intersection using Bézier clipping, *Comput. Aided Design*, **22** (1990), 538–549. https://doi.org/10.1016/0010-4485(90)90039-F

39. C. Y. Hu, T. Maekawa, E. C. Sherbrooke, N. M. Patrikalakis, Robust interval algorithm for curve intersections, *Comput. Aided Design*, **28** (1996), 495–506. https://doi.org/10.1016/0010-4485(95)00063-1

40. C. Schulz, Bézier clipping is quadratically convergent, *Comput. Aided Geom. Design*, **26** (2009), 61–74. https://doi.org/10.1016/j.cagd.2007.12.006

41. G. Jaklič, J. Kozak, On parametric polynomial circle approximation, *Numer. Algorithms*, **77** (2018), 433–450. https://doi.org/10.1007/s11075-017-0322-0

AIMS Press

© 2023 the Author(s), licensee AIMS Press. This is an open access article distributed under the terms of the Creative Commons Attribution License (http://creativecommons.org/licenses/by/4.0)